JOURNAL OF MATERIALS SCIENCE 22 (1987) 539–546

Intermetallic phases in the aluminium-side corner of the AlFeSi-alloy system

V. STEFÁNIAY, Á. GRIGER, T. TURMEZEY
Aluterv-FKI, Budapest, H-1389, POB 128, Hungary

Intermetallic phases formed in the aluminium-base alloys of composition 4 to 14 mass % Si and 20 to 35 mass % Fe were studied by electron probe microanalysis and X-ray diffraction. In the non-equilibrium (as-cast) samples θ-AlFe, α-AlFeSi, β-AlFeSi and γ-AlFeSi phases were identified. It was established that the θ-AlFe phase contained 1 to 6% Si causing a change of lattice parameters. In the quasi-equilibrium (heat-treated) state the chemical composition of the α-AlFeSi is within 6 to 9.5% Si and 32 to 36% Fe and that for the β-AlFeSi within 14 to 16% Si and 27 to 28% Fe. On the basis of the chemical compositions of the intermetallic phases, the 600° C isotherm section of the aluminium-side corner of the AlFeSi-system was revised.

1. Introduction

The Al–Fe and AlFeSi intermetallic phases resulting in aluminium alloys are the subject of extensive research because their morphology, crystal structure and chemical composition affect the mechanical properties, corrosion resistance and surface quality of the finished product. Structural investigations of the intermetallic phases, however, are rendered more difficult by various methodological problems, e.g. they are present merely in small quantities, their size does not exceed 1 μm and they are often in the non-equilibrium state. The composition of AlFeSi phases occurring in industrial alloys lies in the range of 40% Fe maximum and 15% Si maximum, further from the aluminium-corner of the AlFeSi system. The investigation of this range is thus justified though alloys of this kind are not being manufactured for industrial purposes.

Although investigation of the AlFeSi system [1] began in 1921, because of its complexity the entire system is still unclear, according to a recent critical study [2]. Construction of the phase diagram is rendered more difficult by the condition that the prevailing peritectic reactions do not take place completely, solidification is of the non-equilibrium character in almost every case, and while carrying out heat treatment the equilibrium state will be approached very slowly.

The range of 0 to 35% Si and 0 to 30% Fe has been investigated by Gwyer and Phillips [3] by means of thermal analysis and optical metallography. Within this range the θ-AlFe, α-AlFeSi, β-AlFeSi and δ-AlFeSi phases have been identified and their primary crystallization range and transformation temperature have been determined. (The phases are designated according to the system of Phillips and Varley [4].) The authors emphasized that the peritectically solidifying phases formed a crust-like encasement around each other thus excluding the earlier solidified phases from the system [3]. Therefore, in the cast state, more phases may exist simultaneously than ought to be possible according to the phase rule in equilibrium.

Construction of the phase diagram of the AlFeSi-system is associated with Takeda and Mutsuzaki [5]. They found 6 ternary phases within the system and 19 quaternary invariant points. The equilibrium phase diagram has been demonstrated by a set of isoconcentration curves with the iron content increasing at 5% paces.

Armand [6] distinguished between three independent phases within the α-AlFeSi field and designated them α_1, α_2 and α_3. Contradictions relative to the phases of the AlFeSi-system made, Munson [7], caused revision of the range of 0 to 16% Si and 0 to 12% Fe. In the ternary alloys within the α-field he found two phases which were earlier described by Armand [6] as α_2 and α_3, but he designated them as hexagonal α-AlFeSi and β-AlFeSi. He established that the cubic α-AlFeSi (that is the α_1 phase of Armand) can form in alloys containing small amounts of transition metals (manganese, chromium). Sun and Mondolfo [8] commented on Munson's paper [7], confirming that the cubic α-AlFeSi does not form in a ternary system.

Since in spite of extensive research work done insufficient data are available concerning the crystallization and composition of the AlFeSi-phases, samples containing 4 to 14% Si and 20 to 35% Fe were investigated by means of an electron probe microanalyser and by the X-ray diffraction powder method.

2. Experimental details

2.1. Sample preparation

Composition, determined by the wet chemical analysis, of a set of 4N aluminium-based alloys made by the addition of iron and silicon can be seen in Table I (chemical compositions are given in mass %).

The samples were melted at 100 Pa in a Leybold–Hereaus vacuum induction furnace. The melt was cast in an iron mould 30 mm in diameter with a cooling

0022–2461/87 $03.00 + .12

TABLE I Chemical composition of samples and mass fraction of phases measured by X-ray diffraction

No. of sample	Chemical composition (%)			Mass fraction of phases (%)					
	Fe	Si	Al	α-AlFeSi	β-AlFeSi	γ-AlFeSi	θ-AlFe(Si)	Al	Si
1	22.5	3.9	73.6	40	–	–	25	34	1
1H	22.5	3.9	73.6	49	–	–	18	33	–
2	32.6	3.9	63.5	47	–	–	45	8	–
2H	32.6	3.9	63.5	15	–	–	75	10	–
3	31.1	4.6	64.3	50	–	–	39	11	–
3H	31.1	4.6	64.3	25	–	–	61	14	–
4	17.8	9.7	72.5	2	50	–	8	38	2
4H	17.8	9.7	72.5	–	66	–	–	34	–
4L	19.1	8.7	72.2	–	60	–	8	32	–
5	28.7	14.1	57.2	–	5	75	18	–	2
5H	28.7	14.1	57.2	–	100	–	–	–	–
6	31.5	7.8	60.7	25	25	15	30	5	–
6H	31.5	7.8	60.7	100	–	–	–	–	–
7	32.6	9.4	58.0	–	–	65	20	15	–
7H	32.6	9.4	58.0	89	8	3	–	–	–
8	33.1	11.5	55.4	–	–	86	2	12	–
8H	33.1	11.5	55.4	52	7	41	–	–	–
8L	33.0	11.5	55.5	–	5	57	20	16	2
9	34.9	12.3	52.8	4	–	95	1	–	–

rate of 10 to 15° C $\sec^{-1}$. Samples cooled in the furnace at a rate of 1° C $\sec^{-1}$ were also prepared and they were designated by the letter L. The equilibrium state was approached by heat-treatments carried out at 600° C, however, with samples 1 and 4 at 570° C.

The time of heat-treatment took a maximum of one month and the heat-treated condition is indicated by the letter H. The effect of heat-treatment was investigated on rapidly solidified samples. Flat surface areas were prepared by the usual metallographic polishing method for the purpose of electron probe analysis. For the X-ray diffraction the brittle samples were ground to a grain size of about 40 μm.

2.2. Investigation

Chemical composition of the phases was measured by a computer controlled Jeol-JCXA-733-type electron probe microanalyser. On moving the sample forward step by step at 2 μm paces, quick (0.1 sec) tentative measurements were carried out with fixed focused electron beam. In so far as at the given point the intensity of the *Kα* line of iron exceeds the preset threshold value, quantitative analysis was carried out and the concentration data of 100 to 300 point analyses were stored on disk. This way no measurements were made on the aluminium-matrix, cracks and cavities.

The analytical results were represented in the form of points on the Fe–Si concentration plane (Fig. 1). In the "phase maps" thus constructed in addition to the measurement data, the concentration ranges presumed and the straight lines representing the Fe/Si ratio of the individual phases were also indicated. Based on the highest density of the measuring points in the phase map the phases could be distinguished and their composition limits could be read off.

In the course of quantitative analysis the usual corrections for atomic number and absorption have been made. The accelerating voltage applied was 15 kV and the sample current was 10^{-7} A. The absolute error of the phase composition read off the phase maps was about ±0.5%. Phase morphology was studied by the back-scattered electron images (BEI) and from these the phases could be distinguished on the basis of the average contrast depending on the atomic number.

For the identification of phases and the measurement of their mass fraction the X-ray diffraction powder method was applied. Investigations were made with a Philips diffractometer applying Cu*Kα* radiation. Integrated intensity values corresponding to the individual phases were determined by making weighted averages of the peak area of several characteristic diffraction lines of the phase. For the quantitative measurement of phases, weight factors estimated from several independent measurements were used. Reliability of the quantitative phase analysis was checked by comparing the X-ray diffraction phase analyses and the average data of chemical analyses of the samples. Lattice parameters of the θ-AlFe phase were determined by the method described in [9].

3. Results

3.1. θ-AlFe phase

Based on the BEI made of the as-cast samples (e.g. Fig. 1), it could be established that an iron-rich phase crystallizes from the melt first (light brightness in the BEI) covered with other phases (greyer brightness) less in iron content. In accordance with the results of the X-ray diffraction phase analyses (Table I) and the microprobe phase maps (Table II) this phase, occurring in every as-cast sample, is the θ-AlFe. (It may be described by the formulae Al_3Fe and $Al_{13}Fe_4$.) It can be seen on the phase maps that θ-AlFe dissolves a

TABLE II Chemical composition of intermetallic phases measured by electron probe microanalyser (mass %)

No. of sample	α-AlFeSi		β-AlFeSi		γ-AlFeSi		τ_2-AlFeSi		θ-AlFe(Si)	
	Si	Fe	Si	Fe	Si	Fe	Si	Fe	Si	Fe
1	6–7.5	31–32	–	–	–	–	–	–	1–2	39–40
1H	6–6.5	33–34	–	–	–	–	–	–	1–2	38–40
1L	6–7	31–32	–	–	–	–	–	–	1–5	39–40
2	7–9	33–35	–	–	–	–	–	–	1–2.5	38–42
3	6–7	28–32	–	–	–	–	–	–	1–2	36–38
3H	6–7	34–36	–	–	–	–	–	–	1	40–42
4	9–11	32–34	14–16	25–28	–	–	–	–	3.5–4.5	39–40
4H	–	–	14–16	27–28	–	–	–	–	–	–
4L	–	–	14–15	26–28	–	–	–	–	2–3	38–40
5	–	–	–	–	13–18	31–36	–	–	5–6	36–38
6	8–13	33–35	13	28	?	?	–	–	1.5–3	38–41
6H	7.5–8	33–34	–	–	–	–	–	–	–	–
7	–	–	–	–	9–13	35–37	12–14	42	2–3.5	41
7H	8.5–9.5	33–34	13.5–14.5	27–28	?	?	–	–	–	–
8	–	–	–	–	13–16	35–37	12–14	41	4–4.5	41
8H	8.5–9.5	32–33	13.5	27	11–14	33–36	–	–	–	–
8L	8–10(?)	35(?)	15	27	13–15	35–37	14.5	41	4–5	40
9	–	–	–	–	15–16	33–37	16	40	5–6	35–39
9H	–	–	–	–	14–17	31–36	–	–	4–5	36–39

considerable amount (1 to 6%) of silicon. Therefore, the θ-AlFe phase formed in the AlFeSi samples will later be referred to as θ-AlFe(Si). The silicon content of the θ-AlFe(Si) is diminished during heat-treatment.

It was presumed that silicon in the θ-phase causes the change of lattice parameters. It was known, however, that the change of iron content in θ-AlFe also resulted in a change of lattice parameters [9]. Since this phase also contained silicon the two effects had to be separated. Presuming that the two effects are additive, the lattice parameters corresponding to the iron concentration measured by microprobe have been calculated (Table IIIa). According to this the change of cell parameters, *a* and *b*, and moreover, that of the cell volume, *V*, could be related to the silicon content (Table IIIb), whereas no significant change of parameters *c* and β could be detected. There is a linear relationship between the cell dimension and the silicon content of the θ-AlFe(Si) phase. A straight line has been fitted on the points characterized by double-sided errors. Considering the constants determined earlier [9] the change of lattice parameter caused by iron and silicon, and, moreover, that of the cell volume, can be described by the following additive expression:

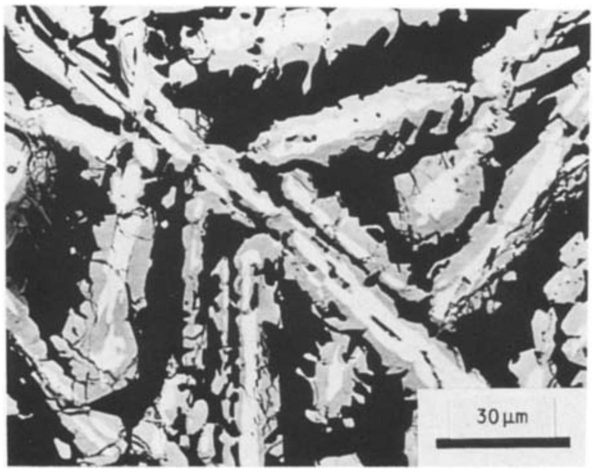

Figure 1 BEI of sample 1 of composition 22.5% Fe, 3.9% Si and 73.6% Al. Identification intermetallic phase: light = θ-AlFe(Si), grey = α-AlFeSi, black = aluminium.

$$a = (15.05 + 1.14 \times 10^{-2}C_{Fe} - 4.1 \times 10^{-3}C_{Si}) \times 10^{-10}\text{mm}$$

$$b = (8.628 - 1.41 \times 10^{-2}C_{Fe} + 1.3 \times 10^{-2}C_{Si} \times 10^{-10}\text{m}$$

$$V = (1572 - 2.16C_{Fe} + 2.7C_{Si}) \times 10^{-3}\text{m}^3$$

In the course of crystallization of primary θ-AlFe(Si) the melt becomes enriched in silicon, and then depending on the bulk composition of the sample, crystallization of various ternary phases starts. Depending on the chemical composition of samples, three secondary AlFeSi phases can be distinguished: the hexagonal α-AlFeSi, the γ-AlFeSi, and a third, assumed to be τ_2-AlFeSi based on the composition, though not proved by X-ray diffraction. Later in this report our samples will be grouped according to the secondary phases.

TABLE III(a) Calculated values of lattice parameters, *a* and *b*, of the θ-AlFe phase as a function of the iron content of the phase [9]

Sample	C_{Fe} (%)	*a* calculated (10^{-9}m)	*b* calculated (10^{-9}m)
9	37 ± 2	1.5477(4)	0.8108(4)
9H	38 ± 1	1.5488(4)	0.8092(4)
4L	39 ± 1	1.5500(5)	0.8076(4)
1L	39.5 ± 1	1.5505(5)	0.8068(4)

TABLE III(b) Change of lattice parameters, *a* and *b*, and lattice volumes, *V*, of the phase θ-AlFe(Si) as a function of the silicon content of the phase

Sample	C_{Si} (%)	a (10^{-9} m)		b (10^{-9} m)		ΔV (10^{-9} m)
		a measured	Δa	b measured	Δb	
9	5.5 ± 0.5	1.5505(5)	−0.0023(5)	0.8038(3)	0.0070(4)	15.6(3)
9H	4.5 ± 0.5	1.5504(8)	−0.0016(8)	0.8040(4)	0.0052(4)	14.9(5)
4L	2.5 ± 0.5	1.5513(3)	−0.0013(3)	0.8040(3)	0.0036(4)	5.9(5)
1L	1.5 ± 0.5	1.5495(3)	−0.0005(9)	0.8050(5)	0.0018(4)	10.4(5)

3.2. The α-AlFeSi phase

The crystallization of θ-AlFe(Si) has been followed by the (hexagonal) α-AlFeSi in samples 1 to 4 of low Fe + Si content. In the BEI made of sample 1 (composition 3.9% Si, 22.5% Fe, Fig. 1) the needle-shaped θ-AlFe(Si) crystals of light brightness are surrounded by α-AlFeSi of greyer brightness. The ternary phases are embedded in the Al-matrix with small amounts of silicon in the latter. During heat-treatment the amount of θ-AlFe(Si) diminished, silicon vanished and the mass proportion of the α-AlFeSi increased. Little change was observed in the morphology of the ternary phases on the effect of heat-treatment, merely the interface between α-AlFeSi and aluminium became more articulated.

The BEI (Fig. 2a) of sample 1L of a nearly similar composition and having been solidified more slowly, has been exposed in such a way that the details of the eutectic solidified at the last could also be observed. (In such a case the iron-containing phases are overexposed.) Lighter grains of smaller size and white needles (iron-rich) can be observed in the aluminium metal of the dark contrast in the image. An X-ray area scan picture of silicon (Fig. 2b) shows that the grains correspond to silicon crystals and the needles to α-AlFeSi phase. The β-AlFeSi component of the Al + Si + β-AlFeSi ternary eutectic, however, was not detected in this sample.

In sample 2 of composition 3.9% Si and 32.6% Fe the θ-AlFe(Si) and α-AlFeSi phases were distinguished which can easily be observed both in the BEI (Fig. 3a) and in the phase map (Fig. 4). During heat-treatment approaching the equilibrium state, the phase interfaces became more rounded off (Fig. 3b), the amount of θ-AlFeSi increased and that of α-AlFeSi decreased. In sample 3 containing slightly more (4.6%) silicon, a microstructure similar to sample 2 developed.

It is equally characteristic of samples 1, 2 and 3 that in the quasi-equilibrium state the Al–θ-AlFe(Si)–α-AlFeSi are arranged in a three-phase field.

In the sample of higher Si/Fe ratio and composition of 9.7% Si and 17.8% Fe, the crystallization of secondary α-AlFeSi is followed by the solidification of a higher amount of β-AlFeSi. Significant phase transformation taking place in the sample during heat-treatment is demonstrated by the phase maps (Fig. 5) of the as-cast and heat-treated samples. In the as-cast (non-equilibrium) state the phases exist over a wide concentration range. The θ-AlFe(Si) and α-AlFeSi possess considerable excess amounts of silicon (Fig. 5a). Owing to the phase interfaces, the analysis points frequently coincided with the boundary of phases. Due to the simultaneous excitation of the two phases, measuring points appeared along the straight lines connecting the phases in the phase map. This effect can be observed clearly along the straight line connecting the aluminium-corner with β-AlFeSi. The points corresponding to the extremely high silicon concentration result from the excitation of silicon grains of the eutectic. During heat-treatment, the θ-AlFe(Si), α-AlFeSi and silicon phases transform to β-AlFeSi, so the sample lies in the Al–β-AlFeSi quasi-binary field (Fig. 5b).

3.3. γ-AlFeSi phase

The crystallization of θ-AlFe(Si) was followed by γ-AlFeSi in sample 5 of composition 14.1% Si and 28.7% Fe. Three phases can be observed in the BEI

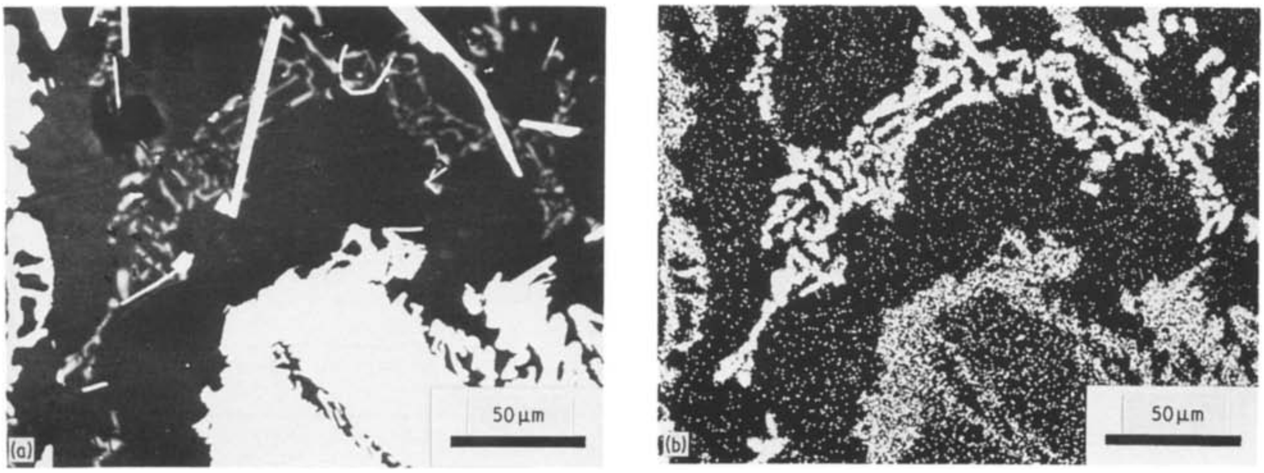

Figure 2 Images of sample 1L of composition 24.2% Fe, 3.6% Si and 72.2% Al. (a) BEI, light = α-AlFeSi, grey = Si, dark = aluminium. (b) Silicon X-ray area scan.

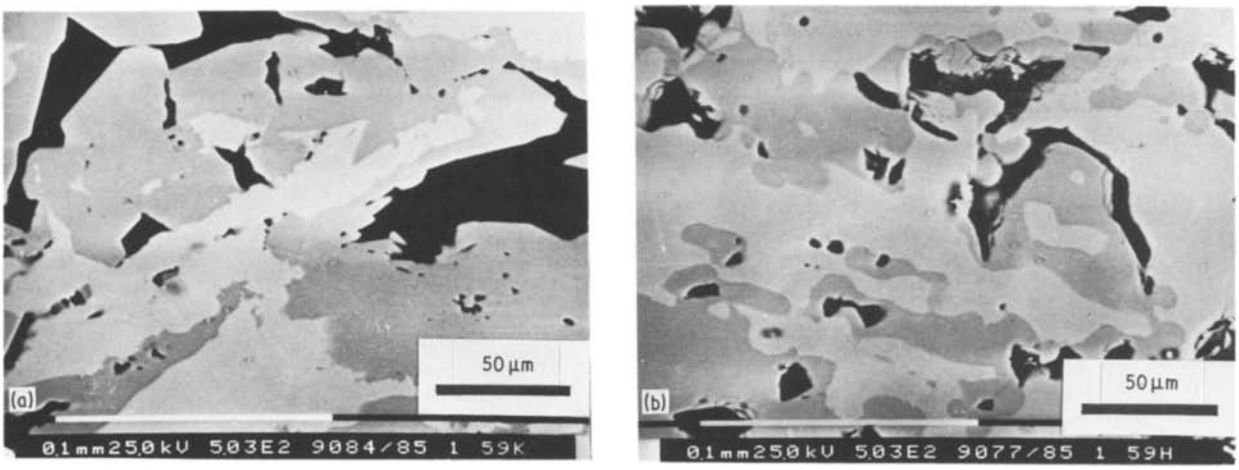

Figure 3 BEI of sample 2 of composition 32.6% Fe, 3.9% Si and 63.5% Al: light = θ-AlFe(Si), grey = α-AlFeSi, dark = aluminium and cavities. (a) As-cast state, (b) heat-treated state.

which correspond to θ-AlFeSi, γ-AlFeSi and β-AlFeSi according to the X-ray diffraction results. From the phase map (Fig. 6) the presence of phases θ-AlFe(Si) having extremely high (5 to 6%) silicon content and γ-AlFeSi can be seen. During heat-treatment, almost the entire alloy transforms into β-AlFeSi.

In sample 6 of composition 7.8% Si and 31.5% Fe containing less silicon compared to the previous sample, γ-AlFeSi in addition to θ-AlFe(Si) and α-AlFeSi could be detected by X-ray diffraction phase analysis. In the BEI and the phase map (Fig. 7a) no γ-AlFeSi was observed. In the equilibrium state the sample is completely transformed into α-AlFeSi (Fig. 7b).

3.4. τ_2-AlFeSi phase

In samples 7, 8 and 9 the primary θ-AlFe(Si) was surrounded by a phase containing as nearly as much silicon as was in γ-AlFeSi, but exceeding the latter by far in iron content. This new phase could clearly be distinguised from θ-AlFe(Si) and γ-AlFeSi in the BEI and phase maps. However, due to the diffuse diffraction pattern of γ-AlFeSi, which was present in high quantities, the phase could not be identified by X-ray diffraction. It is presumed that the unknown phase corresponds to ζ-phase designated by Gwyer and Phillips [3] or K_2-phase by Takeda and Mutsuzaki [5] which we now refer to as τ_2-AlFeSi according to the system of Rivlin and Raynor [2]. In samples 7 (7.8% Si, 31.5% Fe) and 8 (9.4% Si, 32.6% Fe) the θ-AlFeSi, τ_2-AlFeSi and γ-AlFeSi phases were identified. In the BEI of sample 8 (Fig. 8) the following constituents can

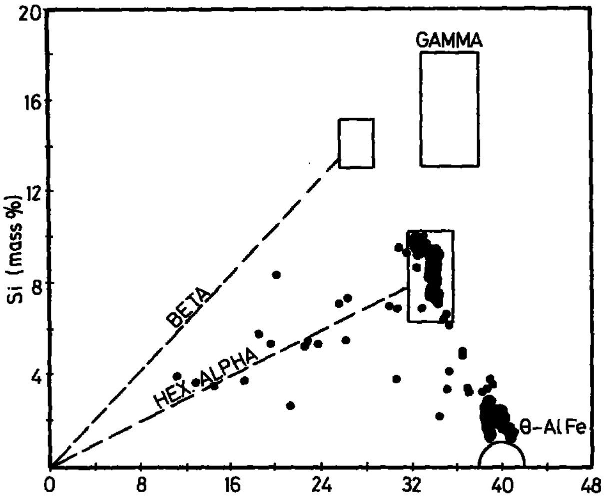

Figure 4 Phase map of sample 2 of composition 32.6% Fe, 3.9% Si and 63.5% Al. Phases: θ-AlFe(Si), α-AlFeSi.

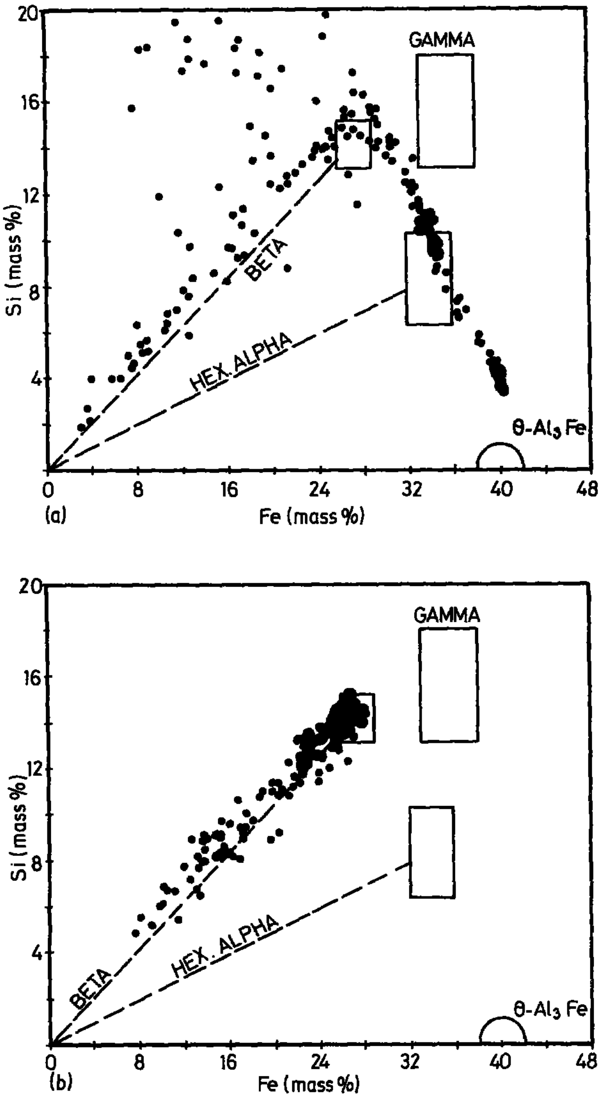

Figure 5 Phase map of sample 4 of composition 17.8% Fe, 9.7% Si and 72.5% Al. (a) As-cast state; phases: θ-AlFe(Si), α-AlFeSi, β-AlFeSi. (b) Heat-treated state; phase: β-AlFeSi.

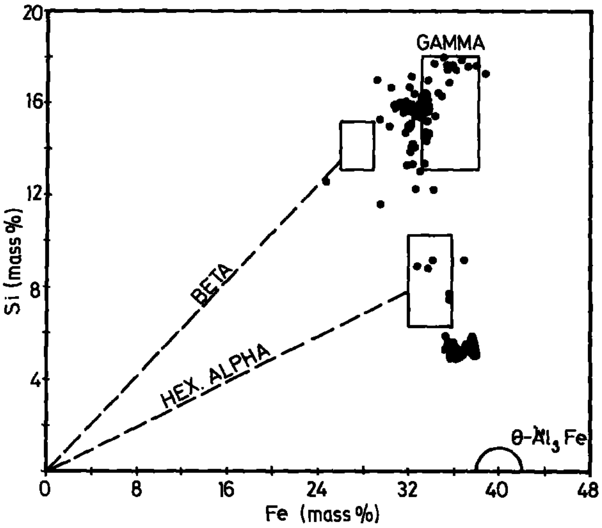

Figure 6 Phase map of sample 5 of composition 28.7% Fe, 14.1% Si and 57.2% Al. Phases: θ-AlFe(Si), γ-AlFeSi.

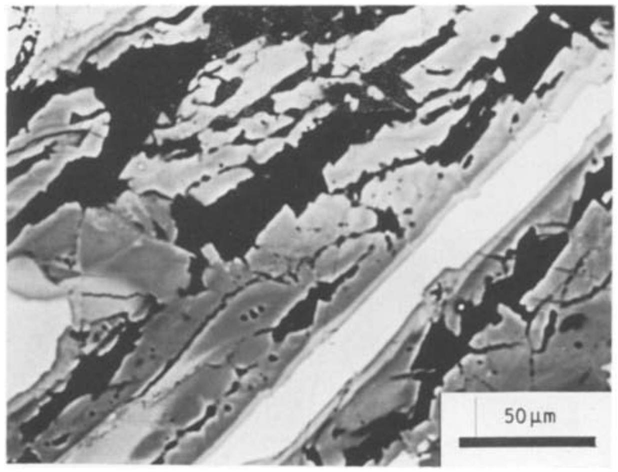

Figure 8 BEI of sample 8 of composition 33.1% Fe, 11.5% Si and 55.4% Al. Identified phases in the image: white = θ-AlFe(Si), light grey = τ_2-AlFeSi, grey = γ-AlFeSi, black = aluminium.

clearly be seen: white elongated θ-AlFe(Si), the τ_2-AlFeSi forming a thin cover around the former and a larger amount of γ-AlFeSi surrounded by aluminium-matrix. In the slower solidifying sample 8L β-AlFeSi is the phase to terminate the solidifying series and based on the phase map (Fig. 9) not even the presence of α-AlFeSi can be precluded. In the equilibrium state the phases of the samples mentioned are in the α-AlFeSi–β-AlFeSi–γ-AlFeSi field. The largest amount of τ_2-AlFeSi phase was in sample 9 containing the highest iron content (34.9% Fe). After heat-treatment in the equilibrium state the sample is in the θ-AlFe(Si)–γ-AlFeSi two-phase field.

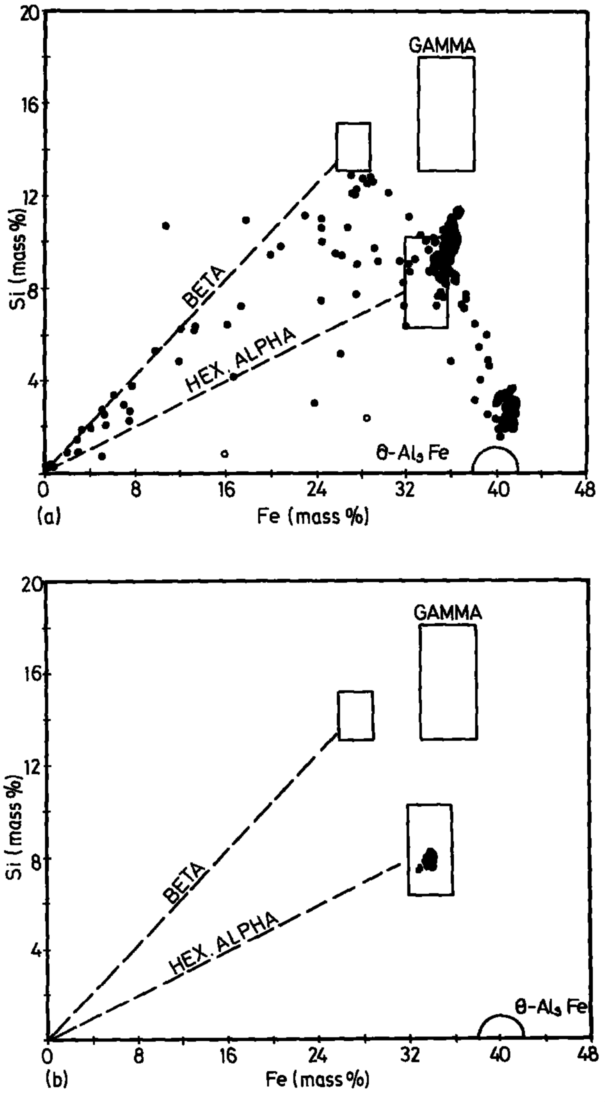

Figure 7 Phase map of sample 6 of composition 31.5% Fe, 7.8% Si and 60.7% Al. (a) As-cast state; phases: θ-AlFeSi, α-AlFeSi, β-AlFeSi. (b) Heat-treated state; phase: α-AlFeSi.

4. Discussion

The points representing the bulk composition of samples indicated on the liquidus area (Fig. 10) of the phase diagram [5, 6] of the AlFeSi system are located in the θ-AlFe field in agreement with our observation according to which the θ-AlFe is the first to crystallize in our samples.

The amount of dissolved silicon found in the θ-AlFe(Si) phase is much higher than was given in earlier publications. Armand [6] found 0.8%, but Sun and Mondolfo [8], however, found only 0.2% of dissolved silicon in the θ-AlFe which had crystallized in the ternary system. Dons [10], however, gave the formula of the θ-$\mathrm{AlFe_{3.3-3.5}FeSi_{0-0.5}}$ in samples

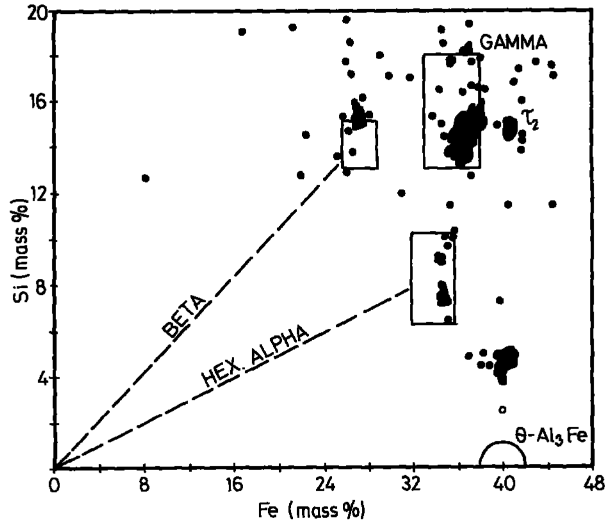

Figure 9 Phase map of the slowly solidified sample 8L of composition 33.0% Fe, 11.5% Si and 55.5% Al. Phases: θ-AlFe(Si), τ_2-AlFeSi, γ-AlFeSi, α-AlFeSi and β-AlFeSi.

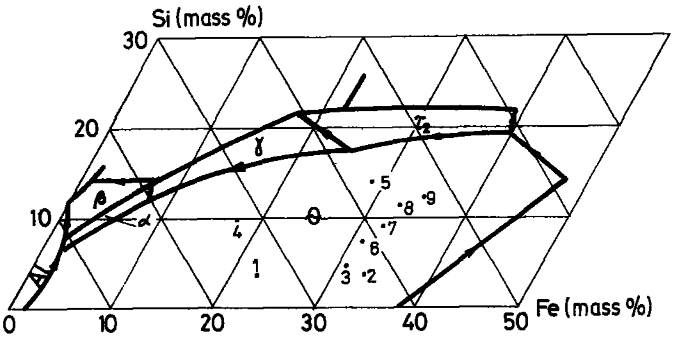

Figure 10 Points indicating the composition of the samples on the liquidus surface of the AlFeSi phase diagram [5, 6].

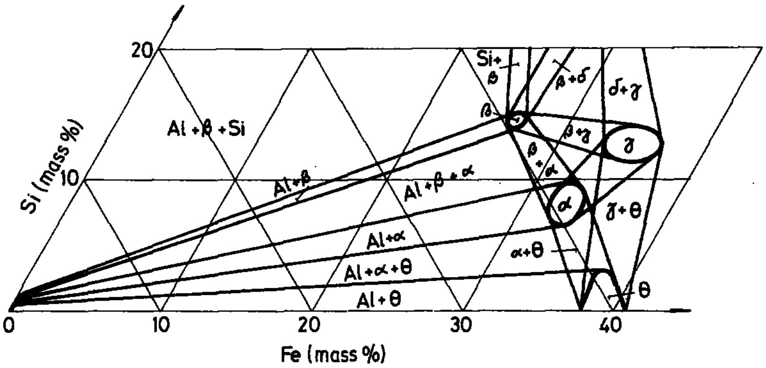

Figure 11 The 570 to 600° C isotherm section of the aluminium-corner of the AlFeSi system based on the present investigations.

crystallized in the low alloy concentration primary aluminium field and Siemensen *et al.* [11] analysed 5% Si in the θ-AlFe phase isolated from samples prepared on commercial purity aluminium.

Dissolved silicon in the θ-phase is also perceivable through its effect on the lattice parameters. With the knowledge of average relative error (0.03%) of the determination of lattice parameters it can be established that the change of parameter *b* is significant because of the change caused by silicon is five times higher than the error of measurement. The situation is similar for the cell volume, whereas the relative change of parameter *a* is commensurable with the average error.

The chemical composition of the AlFeSi phases in the as-cast state extends over wide and partly overlapping ranges (Table IV). The nearly similar chemical composition facilitates the transformations taking place by long-range diffusion which could not have taken place in the course of non-equilibrium solidification.

The hexagonal α-AlFeSi exists in the quasi-equilibrium state in the range containing 6 to 9.5% Si and 32 to 36% Fe. Our results are close to the data (7.4 to 11% Si and 30 to 33% Fe) of Sun and Mondolfo [8] measured by microprobe. Because of the wide composition range the use of a stoichiometric formula is not considered to be justified.

The γ-AlFeSi also has a fairly wide composition range. In the quasi-equilibrium state it occurs in the range 14% Si and 33 to 37% Fe. Armand [6] has measured its large size single-crystal composition to be 12.8% Si and 35.3% Fe falling within the range given by us. According to Sun and Mondolfo [8] and Munson [7], however, the maximum concentration of silicon is 17 to 18%. The difference may originate from the fact that the Fe + Si content of our samples was not sufficiently high.

Rivlin and Raynor [2] have assumed that the ternary phase designated by them as τ_2, corresponding to phase K_2 of Takeda and Mutsuzaki [5], was identical as γ-AlFeSi. According to our measurements, τ_2 is an intermetallic phase different from other ternary phases with a chemical composition of 12 to 15% Si and 40 to 42% Fe. The identity of phases K_2 and ζ seems fairly well established because Takeda and Mutsuzaki and Gwyer and Phillips had found the nearly same temperature of the

$$L + \theta\text{-AlFe} + \tau_2\text{-AlFeSi} \rightleftharpoons \alpha\text{-AlFeSi}$$

quaternary invariant point and that the corresponding liquid composition did not differ.

The range of existence of β-AlFeSi is far narrower: in the quasi-equilibrium state the values 14 to 16% Si and 27 to 28% Fe have been measured. Published data of this phase are also more unanimous: Armand [6] gave 15.2% Si and 26.9% Fe, Black [12] 13.7% Si and 27.2% Fe. Its most probable formula is $Al_9Fe_2Si_2$; however, Al_5FeSi is also being used.

Electron probe microanalysis proved to be a very

TABLE IV Concentration range (mass%) of intermetallic phases measured by the electron probe microanalyser

	α-AlFeSi		β-AlFeSi		γ-AlFeSi		τ_2-AlFeSi		θ-AlFe(Si)	
	Si	Fe	Si	Fe	Si	Fe	Si	Fe	Si	Fe
Non-equilibrium (as-cast)	6–13	31–35	13–16	25–29	9–18	31–37	12–16	40–42	1–6	35–42
Quasi equilibrium (heat-treated at 570 to 600° C)	6–9.5	32–36	14–16	27–28	11–17	31–36	–	–	1–5	36–41

simple and effective method for the determination of the boundaries of the solid phase field of the phase diagram. For example, if a sample according to its average chemical analysis falls on a multi-phase field, then the concentration boundaries of the phase field can be determined by measuring with the microprobe the chemical composition of the phases. At the same time, the equilibrium state of the sample can also be checked on the basis of the homogeneity of the phases.

The 570 to 600° C isotherm section (Fig. 11) in the aluminium corner of the AlFeSi system was constructed on the basis of the concentration of the phases measured in the quasi-equilibrium state. The boundary lines of the phases close to the aluminium corner were drawn from Phillip's data [13]. Considering that liquid phase also exists at 600° C in the Al + β-AlFeSi and Al + β-AlFeSi + Si fields, samples 1H and 4H were heat-treated only at 570° C, i.e. below the temperature of the ternary eutectic.

References

1. W. ROSENHAIN, S. L. ARCHBUTT and D. HANSON, Eleventh Report to the Alloys Research Committee of the Institution of Mechanical Engineers (1921) p. 212.
2. V. G. RIVLIN and G. V. RAYNOR, *Int. Met. Rev.* **26** (1981) 133.
3. A. G. C. GWYER and H. W. PHILLIPS, *J. Inst. Metals* **38** (1927) 29.
4. H. W. PHILLIPS and P. C. VARLEY, *ibid.* **69** (1943) 318.
5. S. TAKEDA and K. MUTSUZAKI, *Tetsu to Hagane* **26** (1940) 335.
6. M. ARMAND, Congrés International de l'Aluminium, Paris, Vol. 1 (Revue de l'Aluminium, Paris, 1955) p. 305.
7. D. MUNSON, *J. Inst. Metals* **95** (1967) 217.
8. C. Y. SUN and L. F. MONDOLFO, *ibid.* **95** (1967) 384.
9. Á. GRIGER, V. STEFÁNIAY and T. TURMEZEY, *Z. Metallkde* **77** (1986) 30.
10. A. L. DONS, *Z. Metallkde* **75** (1984) 170.
11. C. J. SIEMENSEN, P. FARTUM and A. ANDERSEN, *Fresenius Z. Anal Chem.* **319** (1984) 286.
12. P. J. BLACK, *Phil. Mag.* **44** (1955) 401.
13. H. W. PHILLIPS, "Annotated Equilibrium Diagrams of some Aluminium Alloy Systems" (The Institute of Metals, London, 1959) p. 61.

Received 17 March
and accepted 2 June 1986